Dynamics of magnetic-field-induced clustering in ionic ferrofluids from Raman scattering

D. Heinrich
Institut für Festkörperphysik, Technische Universität Berlin, Hardenbergstrasse 36, 10623 Berlin, Germany

A. R. Goñi
ICREA, Institut de Ciència de Materials de Barcelona, Campus de la UAB, 08193 Bellaterra, Spain

C. Thomsen
Institut für Festkörperphysik, Technische Universität Berlin, Hardenbergstrasse 36, 10623 Berlin, Germany

(Received 9 November 2006; accepted 7 February 2007; published online 23 March 2007)

Using Raman spectroscopy, the authors have investigated the aggregation/disgregation of magnetic nanoparticles in dense ionic ferrofluids (IFF) into clusters due to the action of an inhomogeneous external magnetic field. Evidence for changes in particle density and/or effective cluster size were obtained from the variation of the Raman intensity in a time window from 10 s to 10 min for magnetic fields up to 350 mT and at a temperature of 28 °C. Clustering sets in already at very low fields (>15 mT) and the IFF samples exhibit a clear hysteresis in the Raman spectra after releasing the magnetic field, which lasts for many hours at room temperature. The authors determined the characteristic times of the two competing processes, that of field-induced cluster formation and, at room temperature, that of thermal-activated dissociation, to range from 100 to 150 s. © *2007 American Institute of Physics*. [DOI: 10.1063/1.2713112]

INTRODUCTION

Ferrofluids consist of nanometer size magnetic particles such as iron oxide colloidally dispersed in an organic or inorganic carrier liquid. Ferrofluids exhibit peculiar physical and chemical properties,[1,2] with increasing application in mechanical engineering[3] and medicine.[4] Because of the small dimensions of the suspended particles (5–20 nm), they exhibit a single magnetic domain structure and, hence, superparamagnetic behavior in an external magnetic field.[5] At zero field the orientation of the magnetic moments of the particles is at random, resulting in vanishing macroscopic magnetization. An external field orients the particle magnetic moments leading to large saturation values of the magnetization[6] and a strengthening of the dipole-dipole interactions between nanoparticles. Ferrofluids are classified essentially into two groups, ionic ferrofluids[7] (IFF) and surfacted ferrofluids[8,9] (SFF) depending on whether the colloidal stability is provided by electrostatic or steric repulsive interactions, respectively. In recent years, a new class of ferrofluids, which are ultrastable and often biocompatible, have been developed using a combination of both stabilization methods.[10] Depending on the *p*H value of the solvent solution, IFFs are stabilized by charging the magnetic particles electrostatically by transferring protons (H^+) either out from the nanoparticle surface or back to the grains from the acid solvent.[11] In contrast, SFFs rely on the steric repulsion given by a protecting surfactant layer covering the nanoparticles. Typical thicknesses of the surfactant are such that the magnetic particles may come closer together in the case of ionic fluids. As a consequence, an external magnetic field readily induces (metastable) clustering in ionic ferrofluids rather than in surfacted ones.

The formation of structures,[12] clusters,[13] and other more or less ordered chainlike configurations[14,15] in a magnetic field has attracted much attention in the past years due to the large impact that clustering has on many physical properties of the ferrofluids. Furthermore, computer simulations of the field-induced microstructure of ferrofluids and equilibrium properties such as the magnetization were studied theoretically by mean-field models,[16,17] Monte Carlo methods,[18–20] and molecular dynamics simulations.[21,22] Experimentally, the existence of three-dimensional structures formed by the nanoparticles in magnetic fields was detected using birefringence measurements,[23] optical transmission,[24] neutron scattering,[25] and Raman spectroscopy.[26] Interestingly, a comparative Raman study of magnetic-field effects in surfacted as well as ionic ferrofluids demonstrated a very distinct behavior for both kind of fluids.[27] Such preliminary results gave clear indication of hysteretic and metastable effects with time constants in the range of a few minutes to hours for the intensities of Raman spectra in IFF. Those changes were tentatively attributed to dynamical field-induced clustering of magnetic nanoparticles, which occur as the magnetic particles come closer together in the presence of an inhomogeneous field. On these long-time scales there are only few reports concerning the dynamics of ferrofluids in the presence of an inhomogeneous magnetic field. Forced Rayleigh scattering was used to probe the mass dynamics in an acidic and highly concentrated IFF obtaining for the first time an effective mass diffusion coefficient of the nanograins from the characteristic relaxation times of a concentration grating of colloidal particles induced in the ferrofluid by two intense and mutually interfering laser beams.[28] The short-time aggregation dynamics was studied in SFFs by means of turbidity measurements in the case when cluster formation is

reversibly induced by illumination rather than by applying a magnetic field.[29] Characteristic formation times here lie in the range of a few seconds and depend on the absorbed light power and the concentration of the fluid. This method, however, is not suitable for obtaining information on longer-time aggregation phenomena such as the ones triggered by magnetic fields. Very recently, the particle dynamics in Co ferrofluids was studied in an oscillating magnetic field using a new time-resolved stroboscopic neutron-scattering technique.[30] As far as the *slow* magnetic relaxation is concerned, it is found that the magnetic ordering in domains of about 100 nm in size is lost within a few seconds due to the Brownian motion or Néel-type rotation effects.

In this work we have investigated the time evolution of the Raman signal from an aqueous ionic ferrofluid with a concentration of 1 vol % upon switching on and/or off an inhomogeneous magnetic field up to 350 mT. As demonstrated in earlier work,[26,27] the Raman intensity of the water stretching mode can be used as an indicator of the local concentration of magnetic particles under the focus of the microscope, being also sensitive to clustering effects. Upon the sudden switching of the magnetic field, the intensity of the Raman signal of the IFF exhibits a multiexponential behavior with time associated with different dynamical processes induced by the field. Apart from the fast change in particle concentration (time constants between 20 and 40 s) due to the field gradients in the fluid, there exist two competing processes, that of field-induced cluster formation and, at room temperature, that of thermal-activated dissociation. A striking result concerns the large hysteresis observed in the Raman signal if the IFF is exposed to fields larger than 50 mT, which is taken as evidence of the metastable aggregation of nanoparticles into chainlike clusters. The Raman spectra recover their original intensity after hours in the absence of any field or immediately after the ferrofluid has been treated with ultrasound.

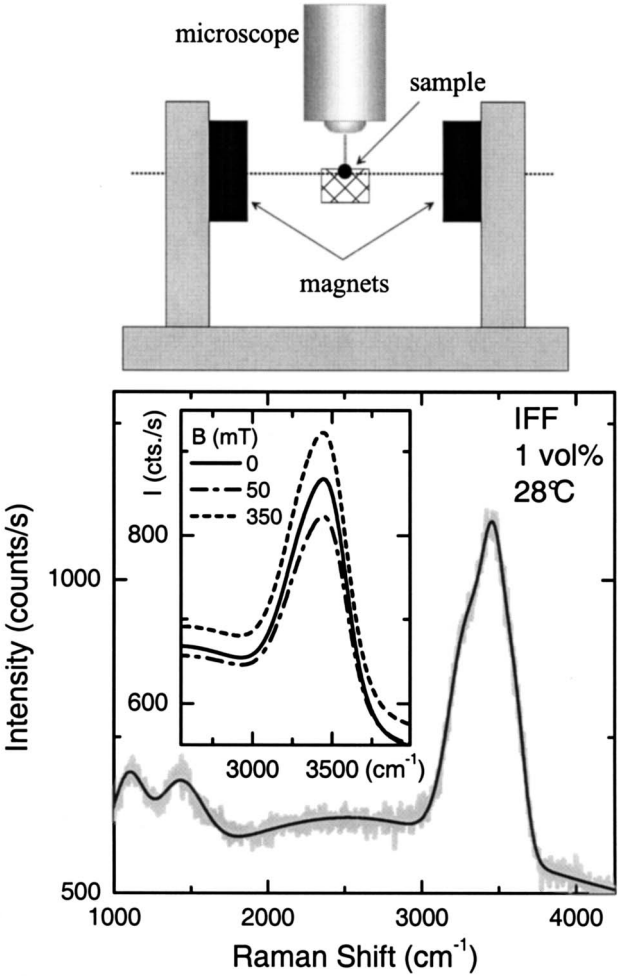

FIG. 1. Upper panel: Sketch of the experimental setup in cross section along the magnetic-field axis. Lower panel: Representative Raman spectrum of a 1 vol % aqueous ionic ferrofluid (IFF) measured at 28 °C and zero magnetic field. The solid curve represents a line-shape fitting function (see text for details). The inset shows three spectra in the energy region of the water stretching mode for different magnetic fields.

EXPERIMENT

The magnetic liquids used in this study are electrostatically stabilized ferrofluids composed of charged magnetite (Fe_3O_4) grains dispersed in water with three different particle concentrations of 1, 0.1, and 0.01 vol %. Nevertheless, since good repeatability of the measurements regarding time-dependent effects is attained only for highly concentrated ferrofluids, we show here exclusively the results obtained for the sample with the highest concentration of 1 vol %. Hydrochloric acid is employed to set pH=3. The average diameter of the grains and agglomerates ranges at around 100 nm.[31] The fluid is loaded into a quartz capillary tube and sealed to avoid evaporation. The integrity of the colloidal suspensions regarding their particle size distribution was checked regularly over the period of months using light scattering methods.

For the Raman experiments we used a single-grating spectrometer equipped with a notch filter for laser-light rejection and a microscope for micro-Raman measurements in backscattering geometry. Spectra were excited with the 514 nm line of an Ar^+-ion laser. Laser powers were kept below 4 mW in order to avoid any annealing process induced by the light excitation. The quartz tubes with the IFF were mounted on a brass block which was kept at a constant temperature between 4 and 60 °C using up to three Peltier cooling units in a series. The external inhomogeneous magnetic field was generated by two permanent supermagnets and was applied perpendicular to the optical axis and to the quartz tube containing the sample. A sketch of the experimental setup is shown in the upper panel of Fig. 1. The laser focus probed always the point of maximum magnetic field at a given pole separation. The strength of the magnetic field was varied by changing the distance between the poles, but for the fast switching of the field the magnets were mechanically removed from or inserted in the microscope setup.

RESULTS AND DISCUSSION

Figure 1 shows a representative Raman spectrum of the aqueous IFF with a concentration of 1 vol % measured at 28 °C with no magnetic field applied. The dominant Raman peak centered at around 3400 cm^{-1} arises from the superposition of the five stretching OH modes of water.[32,33] The solid

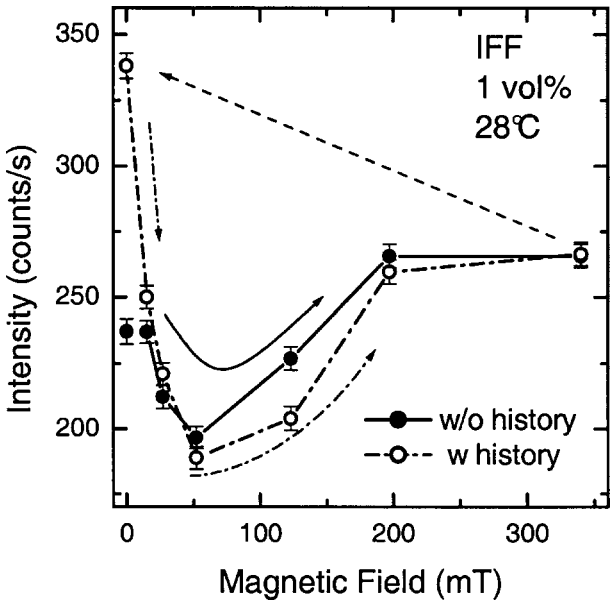

FIG. 2. Raman intensity of the water stretching mode as a function of magnetic field at 28 °C for the cases with (open symbols/dashed line) and without (full symbols and line) previous magnetic-field history. Arrows indicate the sense of variation of the field.

line represents the line-shape fitting function which consists of five Gaussians to describe the OH-stretching modes and a broad Lorentzian background. Throughout the paper, for the analysis of the magnetic-field effects on the Raman spectra *all* peak positions and linewidths were kept constant (their values given by those of the zero-field spectrum). The only free parameters are the peak intensities. The inset in Fig. 1 displays the effect of an external magnetic field on the Raman spectra of the IFF in the spectral range of the OH band. Obviously, the changes in the Raman intensities are due to the presence of the magnetic nanoparticles in the fluid, since no field-induced effects are observed for the solvent solution alone.

The integrated intensity of the Raman band associated with the OH-stretching modes is plotted in Fig. 2 as a function of the applied magnetic field. The measurements were performed in the following way: The field was always increased in steps from zero to 15, 30, 50, 120, 200, and 340 mT. Each data point corresponds to a total measurement time of 3×120 s, and between two consecutive measurements a waiting time of 5 min elapsed. As shown below, the chosen measurement-plus-waiting time is long enough to assure that no appreciable change in intensity occurs. In these experiments we distinguish two situations depending on whether the IFF was or was not previously subjected to a field. This is what we call *field history* hereafter. For the pristine sample without magnetic-field history the behavior of the Raman intensity as the field is increased is represented by the full symbols/solid line in Fig. 2. If after the measurement at 340 mT the field is switched off and the field cycle is started again (always waiting for 5 min in between), the results are surprisingly different, as demonstrated by the open symbols/dashed line in Fig. 2. This *memory* effect in the Raman intensity of the IFF regarding its field history is one of the striking results of this work.

Before discussing the origin of the observed memory effect, we need to take a closer look at the field dependence of the Raman intensity itself. In contrast to what was previously observed for surfacted ferrofluids,[26,27] which in the field range up to 340 mT exhibit a monotonous decrease in Raman intensity, the IFF displays a clear minimum at 50 mT. The steep initial intensity decrease induced by the field occurs for both surfacted and ionic ferrofluids due to the local increase in magnetic-particle concentration. In an inhomogeneous magnetic field such as that in the experiment, the magnetic dipoles of the nanoparticles experience a net force proportional to the local field gradient that drags the particles to higher magnetic-field regions. The result is a symmetrical particle-density distribution along the capillary tube, i.e., in the direction perpendicular to the field produced by the magnets and to the optical axis of the microscope. In fact, we corroborated the existence of such distribution which peaks at the point of highest field (where the laser is focused) by scanning the Raman intensity with the microscope along the tube. The Raman intensity is roughly inversely proportional to the field strength measured with a Hall probe. From our earlier work on SFF with different nanoparticle concentrations,[26] it became clear that this inverse proportionality between particle concentration and Raman intensity results from the field dependence of the scattering volume V and the total number of scatterers N inside V contributing to the Raman signal. The Raman efficiency η for scattering by the OH-mode vibrations is written as[34]

$$\eta=\left(\frac{\omega}{c}\right)^4\frac{V^2N}{A}|\mathbf{e}_i\cdot\tilde{\mathcal{R}}\cdot\mathbf{e}_s|^2, \tag{1}$$

where ω is the frequency of the light, c is its speed in vacuum, A is the cross section of the laser beam, $\mathbf{e}_i$ and $\mathbf{e}_s$ are the unitary polarization vectors of the incident and scattered light, respectively, and $\tilde{\mathcal{R}}$ is the Raman tensor corresponding to the OH-stretching modes of a water molecule. There are two effects which lead to a reduction of η, as the concentration of magnetic particles increases under the focus of the microscope due to the external field. On the one hand, the total number of Raman scatterers N within the scattering volume decreases since water molecules have been displaced away by the magnetic nanograins. On the other hand, the larger the density of nanoparticles, the stronger the Rayleigh scattering,[35] which, in turn, leads to a reduction of the scattering volume. (The darker color of the concentrated ferrofluids is due to stronger Rayleigh scattering rather than absorption!)

Clustering of the magnetic nanoparticles into chainlike agglomerates is the reason for the sudden increase in Raman intensity observed in the IFF above 50 mT (see Fig. 2). At that field the local particle concentration has reached the critical value, for which the attractive dipole-dipole interaction between particles is strong enough to trigger cluster formation. The point is that clustering has also a large impact on the strength of elastic light scattering. Within Mie's theory the balance between the light intensity scattered in the forward direction with respect to the amount of backscattered light depends critically on the parameter $q=2\pi a/\lambda$, where a

is the average radius of the nanoparticles and λ is the wavelength of the incident light.[35] For green/blue excitation (λ =500 nm) we estimate an initial value of $q \sim 0.5$, for which the ratio between forward and backscattering is about unity. If q increases by a factor of 4, the forward scattering becomes two orders of magnitude larger than the backscattering. This results in an effective increase of the scattering volume V available for Raman scattering, which according to Eq. (1) leads to the observed increase in Raman intensity of the IFF above 50 mT. In a process that is comparable to the transition from fog to rain, the generation of big "drops" of particles leads to a marked increase in the scattering volume and thereby in the intensity of the Raman spectra. Such a behavior in the presence of an external field is not observed in SFFs, probably because the thick surfactant layer surrounding the magnetic particles prevents them from getting close enough to form stable clusters.

Cluster formation is also at the origin of the observed memory effect in the Raman intensity, which is apparent only if the highly concentrated IFF was previously subjected to a field $B > 50$ mT. In that case, a certain amount of clusters have been formed, such that at zero magnetic field the scattering volume, i.e., the Raman signal of the OH modes, is larger for the sample with history as compared with that before the first field cycle. We point out that this is a metastable effect. The initial Raman intensity is recovered either after waiting in the absence of any field for several hours (6–8 h) or by immersing the IFF sample in an ultrasonic bath for 3 min. Both treatments promote the disaggregation of the field-induced clusters.

We now turn to the discussion of the time evolution of the Raman signal when a magnetic field is applied to the IFF. For that purpose we measured a series of 20 s long Raman spectra acquired subsequently for a total time of 10 min. An example of the time-dependent changes in the Raman spectra of an IFF sample without previous history induced by turning on a small magnetic field of 30 mT is depicted in Fig. 3(a). The data points represent the integrated intensity of the OH-stretching band for each Raman spectrum of the series, and the solid curve corresponds to the fitting results obtained using a linear combination of simple exponential functions, one for each dynamical process affecting the strength of the Raman signal. The fast decaying exponential term represented by the dashed line corresponds to the sudden increase in nanoparticle concentration caused by the magnetic field. The other two much slower terms, which compete against each other, correspond to the field-induced formation of the nanoparticle clusters (dash-dotted line) and the thermally activated disaggregation process (dash-double-dotted line).

Figure 3(b) illustrates what happens when the field of 30 mT is suddenly removed. The only term reversing its sign is the one of the density change. After switching off the field, the extra attractive interaction between nanograins disappears and the particle concentration at the focus point reduces rapidly. Equilibrium is eventually attained when the concentration of particles is homogeneous throughout the capillary tube. Due to the Mie effect, i.e., the increment of the scattering volume for larger effective sizes of the scatterers, clustering always leads to an increase in Raman intensity, whereas the scattering intensity diminishes due to disaggregation. Of course, in the absence of an external field, the particle aggregation is no longer promoted (the corresponding exponential term vanishes).

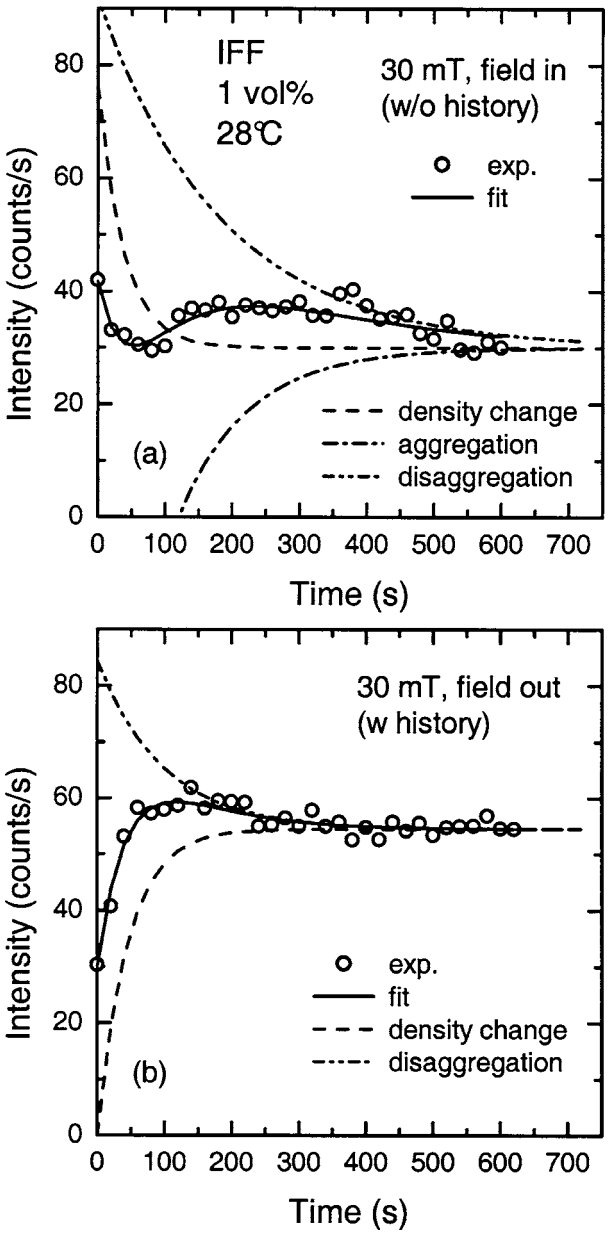

FIG. 3. Time dependence of the integrated intensity of the OH Raman band (open circles) for a 1 vol % IFF at 28 °C when a field of 30 mT is (a) suddenly switched on or (b) switched off. Solid curves are fits to the data points using different exponential functions corresponding to the processes of (dashed line) change in the density of nanoparticles, (dash-dotted line) aggregation, and (dash-double-dotted line) disaggregation.

For further characterization of the dynamical processes which determine the response of the ionic ferrofluid to the influence of external fields, it is very instructive to follow the time dependence of the Raman intensity at different magnetic fields along a typical field cycle, in correspondence with the data of Fig. 2. The intensity transients (symbols) measured at 28 °C when a finite magnetic field is switched on are displayed in Fig. 4(a), whereas the transients acquired when the same magnetic field is switched off are shown in Fig. 4(b). Each sequence of spectra from which we construct

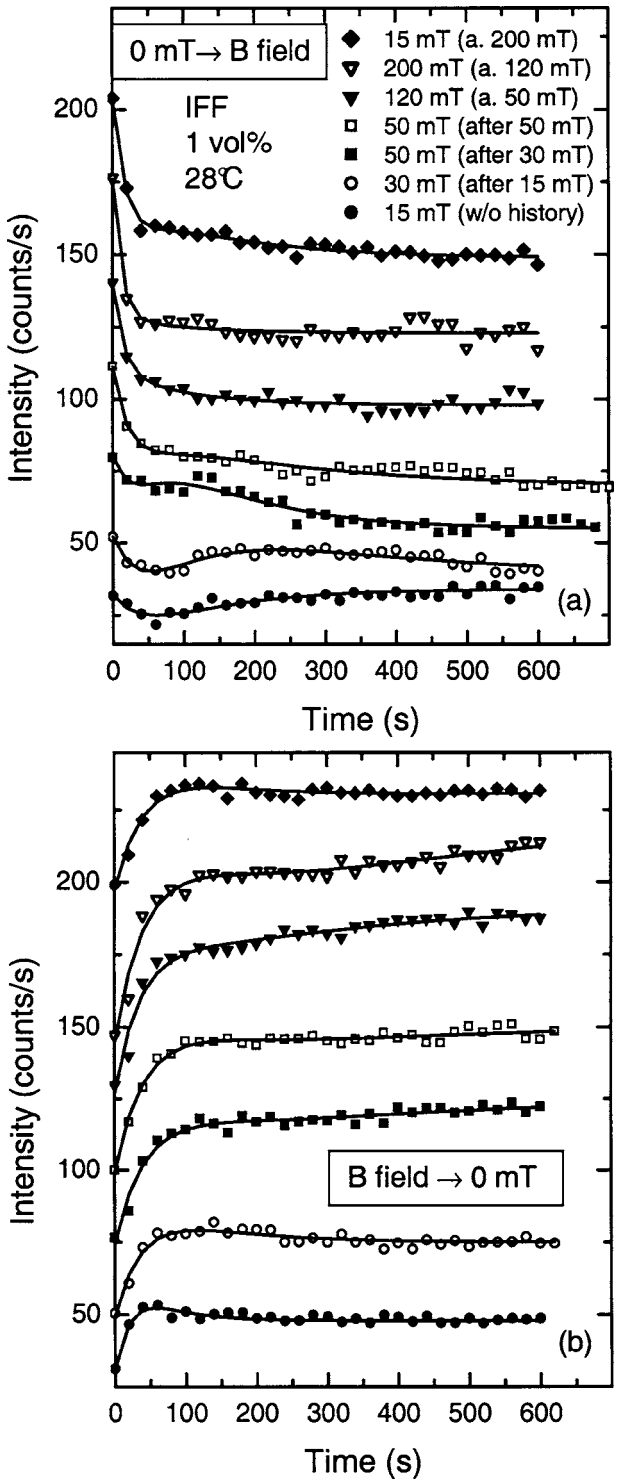

FIG. 4. Time dependence of the integrated intensity of the OH Raman band (symbols) for a 1 vol % IFF at 28 °C for the sudden (a) switching on or (b) switching off of different magnetic fields, as indicated in the legend. Solid curves are fits to the data points using different exponential functions corresponding to the field-induced processes of density change, aggregation, and disaggregation.

the intensity transient has been measured right after the preceding one, i.e., after the IFF was subjected to the previous field. The solid curves are again fits to the data points using linear combinations of exponential functions for the three dynamical processes described above. In Fig. 4(a) we used three exponential functions, two decreasing and one increasing exponentials, corresponding to the change in density and disaggregation and aggregation into clusters. For describing the data of Fig. 4(b), in principle, only two exponentials are required: An increasing one to account for the density reduction and a decreasing exponential to describe cluster disaggregation. Nevertheless, for magnetic fields $B \geqslant 50$ mT an additional increasing exponential is needed to be able to fit the transients at longer times. This cannot be due to clustering since the external field has been switched off. We believe, on the contrary, that this increasing contribution to the Raman intensity stems from the much slower diffusive homogenization of the particle density until reaching equilibrium, which follows after the fast initial decay in concentration.

There are several peculiarities in the nanoparticle dynamics of the IFF which are apparent in the transients of Fig. 4. The first and the last transient at the bottom and the top of Fig. 4, respectively, correspond to the same case of switching on or off a field of 15 mT. The difference, however, is that whereas in the first run the sample had no history, in the last run the sample already experienced a field of 200 mT. For the latter the initial steep intensity change is much more pronounced due to the memory effect and the Raman intensity varies monotonically with time. These effects are a direct consequence of the formation of the clusters induced by the magnetic field. In the sample without history, the nanoparticle clusters start to form immediately after the field has been applied to the IFF. The interplay between the intensity increase due to clustering and the fast intensity decrease imposed by the enhanced concentration induced by the field is responsible for the appearance of a minimum in the transients of Fig. 4(a). At a temperature of 28 °C, however, the disaggregation process plays an important role in the particle dynamics. The evidence that this process is at work is found in the following facts: (i) the incipient maximum observed in the transients obtained when the field is switched off [see Fig. 4(b)] and (ii) the gradual disappearance of the minimum in the transients of Fig. 4(a). In the way the sequence of transients has been subsequently acquired, cluster formation starts to saturate already at low fields, whereas cluster disaggregation gains in importance in inverse proportion. In fact, the second transient measured when the same field of 50 mT is switched on exhibits only a faint minimum, as compared to the previous one. (iii) The 15 mT transient obtained after a magnetic-field cycle has traces of the minimum, implying that the ferrofluid had time to recover, although little, from the clustering induced by the field. In other words, at the temperature of the experiment the IFF partially loses its memory in a time scale of minutes.

Further insight into the dynamical processes induced by an external field is gained from a quantitative analysis of the transients of Fig. 4. From the fitting procedure using simple exponential functions to describe the different aspects of the magnetic-particle dynamics in the IFF, we obtained the time constants plotted in Figs. 5(a)–5(c) as a function of the external field. The shortest time constants correspond to the field-induced change in particle concentration, as displayed in Fig. 5(a) for field switch-on (closed circles) and field switch-off (open symbols). The horizontal lines represent the

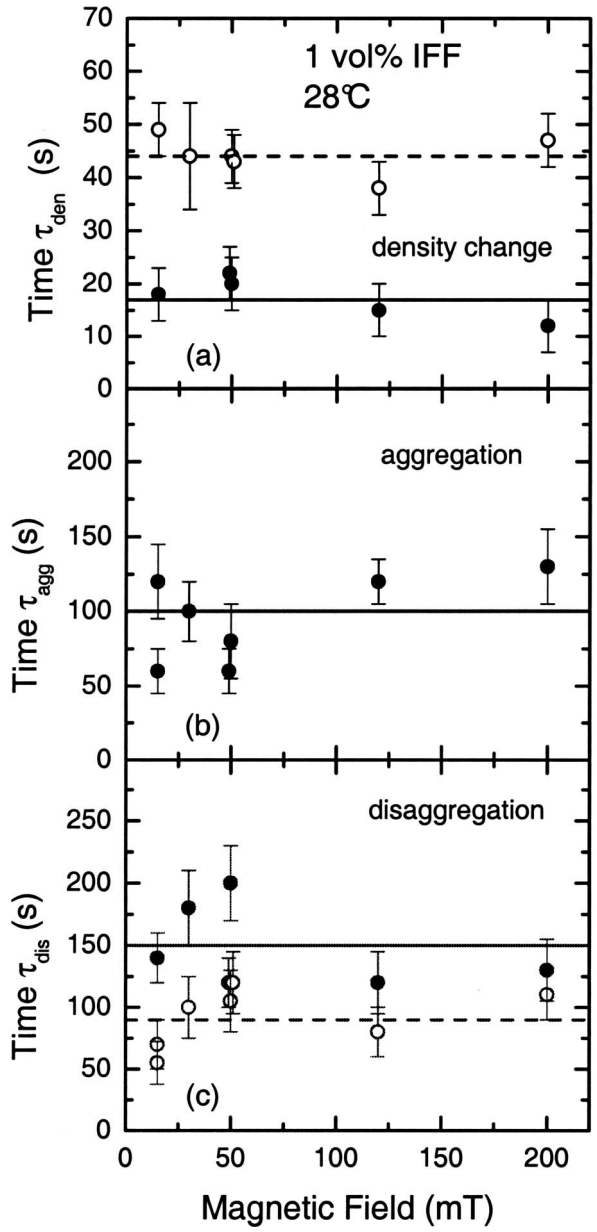

FIG. 5. Time constants as a function of external magnetic field for a 1 vol % IFF at 28 °C corresponding to the processes of (a) change in particle density, (b) aggregation into clusters, and (c) disaggregation of clusters, as determined from fits to the transients of Fig. 4 using exponential functions. Horizontal solid and dashed lines represent the mean values of the time constants corresponding to each process upon switching on (full symbols) and off (open circles) the field, respectively.

mean values of the time constants, which for the switch-on case is $\tau_{den}^{on}=17\pm4$ s. In contrast, when the field is switched off, the nanoparticles need on the average twice as much time to separate with a mean time constant of $\tau_{den}^{off}=44\pm4$ s. This large difference might be explained by taking into account that the long-ranged magnetic dipole-dipole interaction between particles is attractive and is enhanced by the orientation of the dipoles along the external magnetic field. Hence, interparticle interaction could act against dissociation slowing down the process of particle-density homogenization after the magnetic field disappears. Another possibility is that the difference in the time constants for field-switch on/off is due to magnetophoresis, i.e., the favored motion of magnetic grains and agglomerates in field direction, when it is being switched on. We are not able to distinguish between both effects with the data at hand. Further experiments are needed to clarify this point.

Figure 5(b) shows the time constants obtained from the exponents of the increasing exponential function associated with the aggregation of magnetic particles in the ferrofluid when the field is switched on. Despite the scatter of the data we can characterize the aggregation process by having an average time constant of $\tau_{agg}^{on}=100\pm30$ s. The competing process of disaggregation is as fast as the aggregation but when the magnetic field is switched off ($\tau_{dis}^{off}=90\pm20$ s). Interestingly, disaggregation becomes slower in the presence of the magnetic field since the characteristic decay time of the clusters is $\tau_{dis}^{on}=150\pm30$ s. This is again a consequence of the residual attractive interaction between the magnetic dipoles of the nanoparticles, which is enhanced by the external field due to the reorientation of the dipoles along it. All results presented here correspond to room temperature, but it is expected that the nanoparticle dynamics in IFFs should strongly depend on temperature. Such kind of systematic experiments are under way.

CONCLUSIONS

We have investigated the dynamics of clustering in ionic ferrofluids induced by an inhomogeneous external magnetic field using Raman spectroscopy. The evidence for clustering is the metastable change of the Raman intensity of the OH-stretching vibrations of the water molecules caused by variations in the effective scattering volume due to the Mie effect. For magnetic fields larger than 50 mT and at 28 °C the cluster formation is metastable; i.e., the ferrofluid exhibits a memory of the magnetic fields at which it was exposed. The ferrofluid recovers its original state after several hours in the absence of a field or if it is immersed in ultrasonic bath. Furthermore, we were able to determine the characteristic times for the different dynamical processes taking place in the ionic ferrofluid induced by an inhomogeneous external field, namely, the change in particle concentration and the aggregation/disaggregation of the magnetic nanoparticles into/of clusters. The former process is the fastest with time constants of a few tens of seconds. Formation or dissociation of clusters proceed at a lower pace of around 100 s. In this way, we have obtained important quantitative information about the field-induced nanoparticle dynamics in highly concentrated aqueous ferrofluids, which might have large impact on the various applications of these colloidal multifunctional kind of materials.

ACKNOWLEDGMENTS

The authors are grateful to S. Hess and P. Ilg for helpful discussions. Special thanks are due to N. Buske for producing and providing the ferrofluids used in the experiments.

[1] E. Blums, A. Cebers, and M. M. Maiorov, *Magnetic Fluids* (Walter de Gruyter, Berlin, 1997).
[2] H. E. Horng, C.-Y. Hong, S. Y. Yang, and H. C. Yang, J. Phys. Chem. Solids **62**, 1749 (2001).
[3] B. M. Berkovsky, V. F. Medvedev, and M. S. Krakov, *Magnetic Fluids,*

Engineering Applications (Oxford University, Oxford, 1993).
[4] C. Alexiou, W. Arnold, P. Hulin, R. Klein, A. Schmidt, C. Bergemann, and F. G. Parak, Magnetohydrodynamics **37**, 3 (2001).
[5] C. P. Bean and J. D. Livingstone, J. Appl. Phys. **40**, 120S (1959).
[6] R. E. Rosensweig, *Ferrohydrodynamics* (Dover, New York, 1997).
[7] R. Massart, IEEE Trans. Magn. **17**, 1247 (1981).
[8] S. Papell, U.S. Patent No. 3,215,572 (2 November 1965).
[9] N. Buske, Prog. Colloid Polym. Sci. **95**, 175 (1994).
[10] P. C. Morais, R. L. Santos, A. C. M. Pimenta, R. B. Azevedo, and E. C. D. Lima, Thin Solid Films **515**, 266 (2006).
[11] F. Qu and P. C. Morais, J. Chem. Phys. **111**, 8588 (1999); J. Phys. Chem. B **104**, 5232 (2000).
[12] J. Liu, E. M. Lawrence, A. Wu, M. L. Ivey, G. A. Flores, K. Javier, J. Bibette, and J. Richard, Phys. Rev. Lett. **74**, 2828 (1995).
[13] K. T. Wu, J. Magn. Magn. Mater. **209**, 246 (2000).
[14] A. O. Ivanov, Z. Wang, and C. Holm, Phys. Rev. E **69**, 031206 (2004).
[15] V. S. Mendelev and A. O. Ivanov, Phys. Rev. E **70**, 051502 (2004).
[16] A. Cebers, Magnetohydrodynamics **18**, 137 (1982).
[17] K. Sano and M. Doi, J. Phys. Soc. Jpn. **52**, 2810 (1983).
[18] P. J. Camp and G. N. Patey, Phys. Rev. E **62**, 5403 (2000).
[19] T. Kruse, A. Spanoudaki, and R. Pelster, Phys. Rev. E **68**, 054208 (2003).
[20] H. Morimoto, T. Maekawa, and Y. Matsumoto, Phys. Rev. E **68**, 061505 (2003).
[21] Z. Wang, C. Holm, and H. W. Müller, Phys. Rev. E **66**, 021405 (2002).
[22] J. P. Huang, Z. W. Wang, and C. Holm, Phys. Rev. E **71**, 061203 (2005).
[23] E. Hasmonay, E. Dubois, J. -C. Bacri, R. Perzynski, Y. L. Raikher, and V. I. Stepanov, Eur. Phys. J. B **5**, 859 (1998); See also simulations in A. O. Ivanov and S. S. Kantorovich, Phys. Rev. E **70**, 021401 (2004).
[24] G. N. Rao, Y. D. Yao, Y. L. Chen, K. T. Wu, and J. W. Chen, Phys. Rev. E **72**, 031408 (2005).
[25] A. Wiedenmann, J. Magn. Magn. Mater. **272–276**, 1487 (2004).
[26] J. E. Weber, A. R. Goñi, D. J. Pusiol, and C. Thomsen, Phys. Rev. E **66**, 021407 (2002).
[27] J. E. Weber, A. R. Goñi, and C. Thomsen, J. Magn. Magn. Mater. **277**, 96 (2004).
[28] J. C. Bacri, A. Cebers, A. Bourdon, G. Demouchy, B. M. Heegaard, and R. Perzynski, Phys. Rev. Lett. **74**, 5032 (1995).
[29] R. R. Kellner and W. Köhler, J. Appl. Phys. **97**, 034910 (2005).
[30] A. Wiedenmann, U. Keiderling, K. Habicht, M. Russina, and R. Gähler, Phys. Rev. Lett. **97**, 057202 (2006).
[31] N. Buske, Private communication (unpublished).
[32] D. M. Carey and G. M. Korenowski, J. Chem. Phys. **108**, 2669 (1998).
[33] P. C. Morais, S. W. da Silva, M. A. G. Soler, M. H. Sousa, and F. A. Tourinho, J. Magn. Magn. Mater. **201**, 105 (1999).
[34] P. Y. Yu and C. Cardona, *Fundamentals of Semiconductors* (Springer, Berlin, 1996).
[35] M. Born and E. Wolf, *Principles of Optics* (Pergamon, Oxford, 1964).